Functional Materials 20, No.3 (2013)

Radiation resistance of Ti–20Zr alloy in microcrystalline and nanocrystalline state

V.A.Belous, O.V.Borodin, V.V.Bryk, R.L.Vasilenko, V.N.Voyevodin, A.S.Kuprin, V.D.Ovcharenko, E.N.Reshetnyak, G.N.Tolmachova

National Science Center "Kharkiv Institute of Physics and Technology", Kharkiv, Ukraine

Received February 19, 2013

In this work we studied structure of Ti–20Zr alloy in recrystallized and nanocrystalline conditions before and after irradiation by Zr^{3+} ions with energy 1.8 MeV to 80 dpa at 500°C. By transmission electron microscopy methods it was showed that irradiation of the alloy in the recrystallized state induced formation of <*c*> type dislocation loops, which are common characteristic of accelerated radiation-growth of the materials with hcp lattice. Irradiation of the nanostructured material leads to an isotropic increase in the grain size (from 49 nm to 146 nm); the signs of accelerated radiation-growth were not detected.

Проведено сравнительное изучение структуры сплава Ti–20Zr в рекристаллизованном и нанокристаллическом состояниях до и после облучения ионами Zr^{3+} с энергией 1,8 МэВ до 80 сна при температуре 500°С. Методами просвечивающей электронной микроскопии показано, что при облучении сплава в рекристаллизованном состоянии образуются дислокационные петли <*c*> типа, являющиеся характерным признаком ускоренного радиационного роста, свойственного материалам с ГПУ решеткой. Облучение материала в наноструктурном состоянии приводит к изотропному увеличению размеров зерна (с 49 нм до 146 нм), признаков ускоренного радиационного роста не обнаружено.

Радіаційна стійкість сплаву Ti–20Zr у мікрокристалічному та наноструктурному стані. *В.А.Білоус, О.В.Бородін, В.В.Брик, Р.Л.Василенко, В.М.Воєводін, О.С.Куприн, В.Д.Овчаренко, О.М.Рєшетняк, Г.М.Толмачова.*

Проведено порівняльне вивчення структури сплаву Ti–20Zr у рекристалізованому і нанокристалічному станах до і після опромінення іонами Zr^{3+} з енергією 1,8 МеВ до 80 зна при температурі 500°С. Методами просвічуючої електронної мікроскопії показано, що при опроміненні сплаву у рекристалізованому стані утворюються дислокаційні петлі <*c*> типу, які є характерною ознакою прискореного радіаційного росту, властивого матеріалам з ГПУ граткою. Опромінення матеріалу у наноструктурному стані призводить до ізотропного збільшення розмірів зерна (з 49 нм до 146 нм), ознак прискореного радіаційного росту не виявлено.

1. Introduction

Titanium α-alloys are the most prospective material for the new generation of water-water nuclear power plants of different power with increased service life to 60 years and more. These alloys are attractive because their radiation resistance and swelling, activation, mechanical properties, corrosion resistance and other service characteristic may guarantee the required long-term reliability, stability and ecological safety of the prospective power plants [1]. The possibility to reduce the mass of constructions made of titanium alloys is of spe-

cial interest for sea and other transport power plants [2]. Increase of demands to the safety and resource of the nuclear power plants challenges the necessity to develop materials of higher radiation resistance.

One of the prospective way for realization of this task is creation of nanostructure in the material. Such nanomaterials demonstrate the increased radiation resistance in comparison with microcrystalline analogues [3, 4]; this is due to high number of grain boundaries which are the effective sinks of point defects produced under irradiation. It is shown in [5] that nickel radiation defects were not observed in the nanocrystalline after irradiation by Ni^+ ions with energy 840 keV to 5 dpa; in the microcrystalline materials such defects were detected. In [6] authors have showed that fine-grained alloy TiNi with the grain size in the range 20–30 nm under irradiation with Ar^+ ions with energy 1.5 MeV at room temperature to 5.6 dpa keeps the long-range order and doesn't amorphise unlike the coarse crystalline analogue. In [7] the influence of ion irradiation (500 keV — Ar^+, 1 MeV — Kr^+) under doses up to 75 dpa is revealed only on the kinetics of grains growth of nanocrystalline metals (Zr, Cu, Pt, Au) and of alloys Zr–Fe, Cu–Fe.

In the presented paper the radiation damage of alloy Ti–20Zr in different structure states was investigated after ion irradiation.

2. Experimental

Alloy Ti–20Zr of vacuum-arc remelting was rolled to the thickness 0.4 mm and was annealed in vacuum during 30 min at 800°C. After annealing the specimens were thinned by chemical polishing to the thickness 200 μm in electrolyte 45 % of H_2O, 45 % of HNO_3, 10 % of HF.

Nanocrystalline state was formed by vacuum-arc deposition on the equipment "Bulat" composed by two oncoming separated of macroparticles flows of titanium and zirconium plasma [8]. Coatings with thickness 3 μm were deposited on the specimens of recrystallized alloy Ti–20Zr for study of radiation resistance and on stainless steel for X-ray diffraction analysis. The primary coatings were also annealed in vacuum at temperature 500°C during 1 h for separation of structural variations occurring in condensates after annealing and irradiation. Discs with diameter 3 mm standard for investigation of radiation damage by the method of ion irradiation and for transmission electron microscopy were cut out from the material prepared for study of radiation resistance.

Irradiation of the materials in recrystallized and nanostructural states was carried out on accelerator "ESUVI" by Zr^{3+} with energy 1.8 MeV at temperature 500°C to the dose 80 dpa. Under ion irradiation the radiation damage is produced inhomogeneously by the depth therefore the layer for investigation was selected so as to avoid the influence of surface on the one hand and to avoid the influence of interstitial atoms of irradiating substance deposited in the material on the other hand. To remove a part of irradiated layer from the surface the method of jet electropolishing with pulsed current supply was used. The removal of near surface alloy with thickness 100 nm was performed on the set Tenupol-5 in electrolyte 90 % of CH_3OH, 10 % $HClO_4$ under voltage 75 V at temperature of electrolyte — 50°C. The set Tenupol-5 was equipped by the system of current stabilization and by controller of pulse supply. After the removal of the necessary layer the irradiated surface was coated by protective varnish Lakomit and the specimen was subjected to the jet electropolishing on opposite (unirradiated) side until the hole formation. Structure of the specimens was studied on the electron microscope JEM 100CX.

Phase composition and substructure of the specimens were studied by of X-ray diffraction analysis method using diffractometer DRON-3 in filtered radiation of copper anode. Survey of diffractograms for the phase analysis was carried out in the circuit θ–2θ of scanning using Bregue-Brentano focusing in the range of angles from 20 to 130 degrees. Processing of the diffractograms was performed by computer program New Profile. Determination of the size of the range of coherent scattering in the specimens was performed by two processes: using Sherrer formula (L_m) and by the approximation (L_a) [9, 10]. Koshi function was used as an approximation function. After the primary processing of the diffractograms, doublet extraction, an approximation, consideration of an instrument broadening of standard, size and deformation contribution in physical broadening of β lines was separated by plotting of the Hall graphs in coordinates of β–$\cos\theta$–$\sin\theta$.

Composition of the coating was determined by X-ray fluorescence and energy dispersion methods, nanohardness was meas-

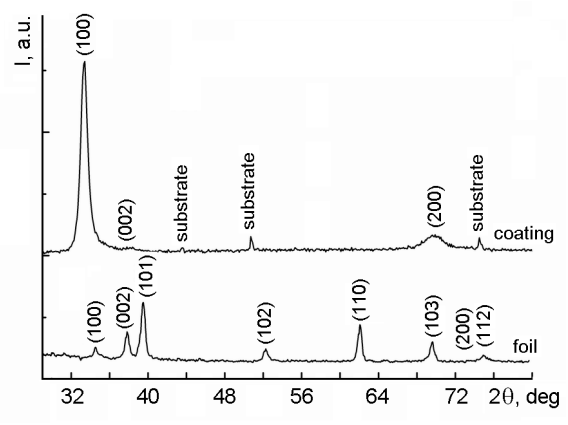

Fig.1 X-ray diffraction of the alloy and the coating system Ti-Zr, which identifies lines of solid solution α-(Ti, Zr).

ured on Nanoindenter G200 by Berkovich indentor using CSM method up to the depth of indentation ~300 nm.

3. Results and discussion

3.1. Structure characteristics of primary specimens

It is known that system Ti–Zr is characterized by a complete solubility of the components [11]. According to the data of X-ray crystal analysis the studied specimens of foils and coatings of the system Ti–Zr have the one-phase structure that represents solid solution α–(Ti, Zr). Diffractogram of the studied specimens are presented in Fig. 1. It is seen that the diffractogram of the foil shows all lines characteristic for the solid solution with hcp structure and the relationship of line intensity doesn't deviate from the values presented for non structurized material. Parameters of crystalline lattice of the solid solution were determined according to the angle positions of lines (002) and (110), they are presented in Table 1. The obtained parameters are rather close to the values calculated by Vegard law for period of solid solution lattice α-(Ti, Zr) with zirconium content 12 at % (that corresponds to 20 %): a = 0.474 nm, c = 0.298 nm.

Alloy Ti–20Zr in initial state has coarse grained structure with low density of intragrained dislocation (according to the data of transmission electron microscopy) (Fig. 2a). In nanocrystalline state the mean size of grain is ~49 nm (Fig. 3a, b). The high density of dislocations is observed inside the grains. Annealing of the condensate at 500°C during 1 h doesn't cause the increase of the grain size. The mean size is 45 nm (Fig. 3c, d) that is equivalent to 45 nm taking into account 10 % error of electron microscopic study. Contrast in the grain body gives evidence about the presence of significant stresses in the coating material.

Determination of parameters of the solid solution substructure in the foil was carried out by the method of approximation for broadening of all available intense diffraction lines. It turned out that despite the absence of lines which are different orders

Table 1. Results of X-ray diffraction patterns of α–(Ti, Zr) alloy and coating

Sample	a, nm	c, nm	L_{Sh}, nm	L_a, nm	ρ, cm^{-2}
Foil	0.299	0.476	24	27	$5 \cdot 10^{10}$
As deposited coating	0.311	–	12	–	–
Annealed coating	0.309	–	14	30	$4 \cdot 10^{11}$

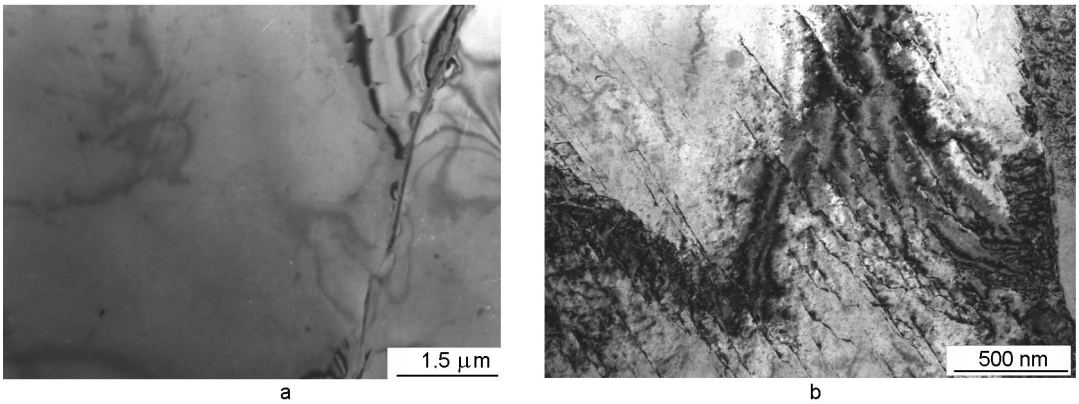

Fig. 2. TEM images of Ti–20Zr alloy in the initial state (a) and after exposure to 80 dpa at 500°C (b).

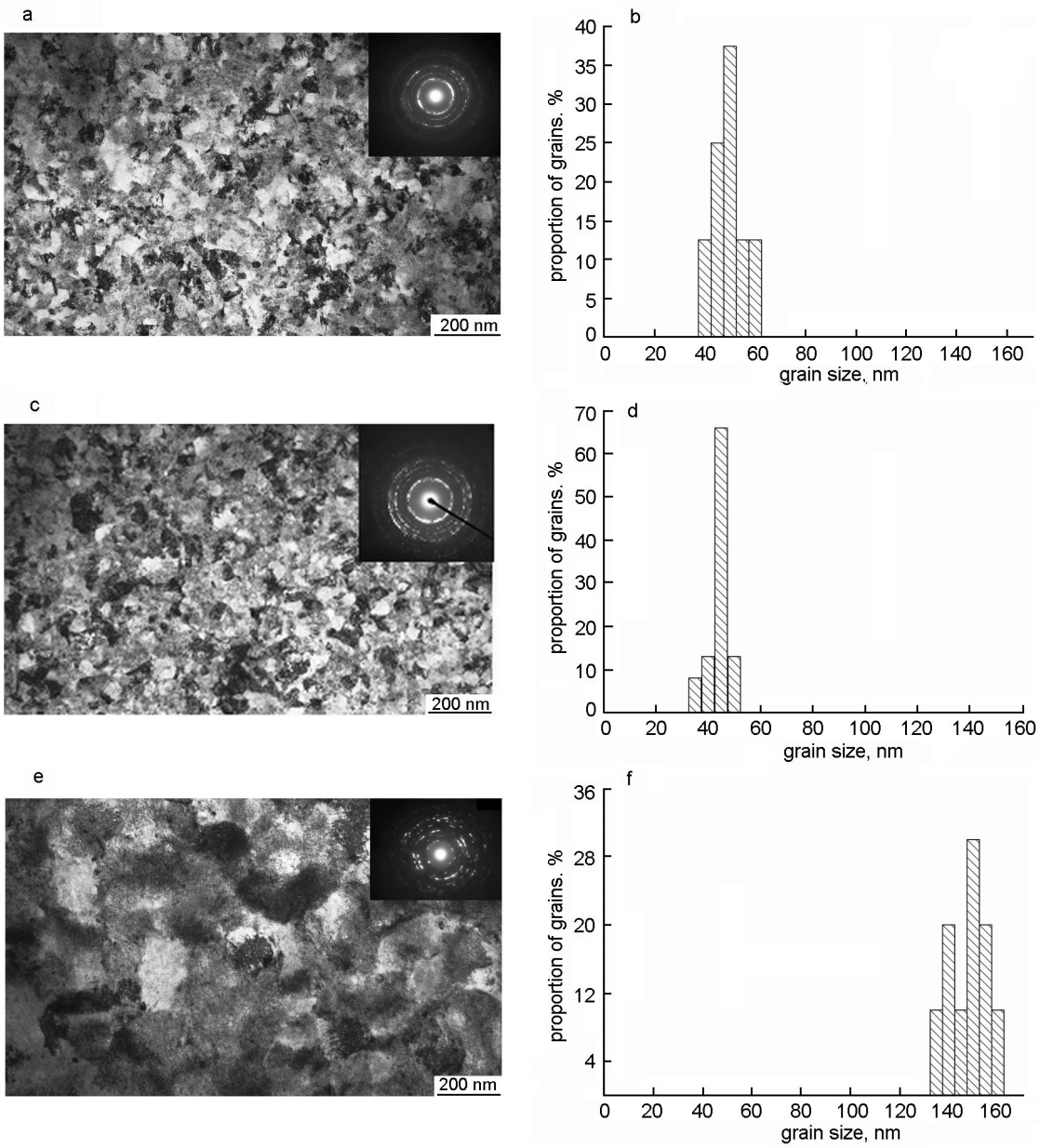

Fig. 3. TEM images and histograms of the grain sizes of nanocrystalline Ti–20Zr after deposition (a, b), after annealing at 500°C (c, d) and after irradiation to 80 dpa at 500°C (e, f).

of one reflection, point on the plot of Hall fall on a straight line (Fig. 4) and the size factor contributes mainly to the broadening of the diffraction lines. According to the results of calculation the size Lm in the foil constitutes 27 nm which practically coincides with value 24 nm (the value obtained with Cherrer formula for line (100)). The level of microdeformation in the foil doesn't exceed 0.06 % which corresponds to the density of randomly distributed in L_m dislocations $7{\cdot}10^9$ cm^{-2}. The mean density of dislocations ρ (see Table 1) according to the data of diffractometry doesn't exceed $5{\cdot}10^{10}$ cm^{-2}.

Unlike the foil on diffractogram of the coatings only two strong lines of the solid solution are seen α–(Ti, Zr):(100) and (200) intensity of these lines is much higher than that of lines for the foil. It is due to formation in the coating of strong texture of axial type with preferred orientation of crystallites by planes (100) in the plane of the base. Lines of the film are significantly broader than lines of the foil and are displaced into the side of lower angles that is caused by the high level of microdeforma-

tion and compressive residual stresses in the film. Compressive stresses cause the significant increase of parameters of crystalline lattice of the solid solution in the direction of normal to the film surface to $a = 0.311$ nm. Crystallite size calculated by broadening of line (100) constitutes 12 nm which is much lower than value obtained by electron microscopy.

For the material in nanocrystalline state we have tried to determine separately the dimensions of the areas of coherent diffraction and microdiffractions in the solid solution crystallites according to the broadening of diffraction lines (100), (200) and (300). The level of crystalline lattice distortion in the film is significantly higher than that in the foil. It is seen on the plot that it is not possible to use the approximation method for separation of dimensions and deformation contribution to the broadening for the primary coating because the condition

$$\frac{\cos\theta_{(100)}}{\cos\theta_{(300)}} < \frac{\beta_{(300)}}{\beta_{(100)}} < \frac{\mathrm{tg}\theta_{(300)}}{\mathrm{tg}\theta_{(100)}} \qquad (1)$$

is not satisfied and the plot of Hall cuts the ordinate axis below zero. Such a singularity of the plot is often observed in the coatings deposited from the flows of accelerated ions and demonstrates the presence of additional factors of line broadening and extremely high presence of defects in the crystalline lattice of the film [12, 13]. According to [14] interstitial atoms may be such defects; they were formed by ion bombardment during deposition [15].

It was established that vacuum annealing of the coating doesn't cause the changes of phase composition and texture in the film but contributes to the partial relaxation of the micro- and macrodeformation. The general view of diffraction pattern doesn't change but lines α–(Ti, Zr) become stronger, narrow and displace towards higher angles. The period of the solid solution lattice in the annealed film decreases to 0.309 nm which is due to anneal of residual stresses.

The Hall plot plotted for annealed coating intersects the ordinate axis higher the zero. The level of microdeformation in the coating calculated by the plot slope is 10 times higher than in the foil, but considerably lower than into the initial coating. This corresponds to the high density of randomly distributed dislocations $6 \cdot 10^{11}$ cm^{-2}. Crystallite dimension α–(Ti, Zr) is equal to 30 nm that is twice higher than values calculated by broadening of the line (100), but is near to the values of the mean size of the grains obtained in the electron-microscopic images.

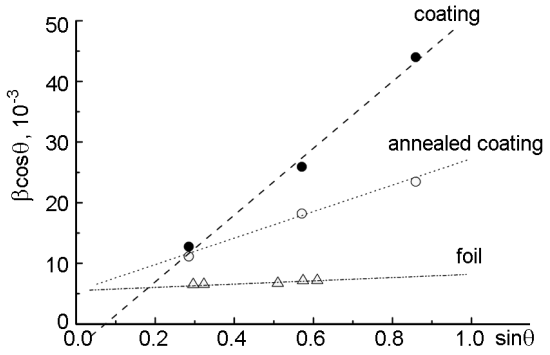

Fig. 4. Hall graphs of α–(Ti, Zr) alloy and coating.

So, it is shown that the structure of the foil and of coating specimens of the system Ti–20Zr prepared for the radiation resistance tests have considerable differences. The foils are composed of micron grains of solid solution α–(Ti, Zr) which have block structure with the block size fractions of μm and sufficiently perfect structure inside the block. Coatings α–(Ti, Zr) are nanocrystalline and are characterized by high density of defects of the crystalline structure. The obtained results demonstrate again that for the correct determination of dimension characteristics of the nanostructural materials a complex study is necessary by methods of electron microscopy and X-ray diffraction analysis [16].

3.2. Change of the structure and mechanical characteristics of specimens after irradiation

After irradiation in the structure of recrystallized alloy elliptic dislocation loops of *a*-type with mean size of 11 nm are present; elements of dislocation network and elongated dislocation loops of *c*-type with the length 400 nm are also observed (Fig. 1b). The detected dislocation loops of *c*-type are the characteristic sing of accelerated radiation growth characteristic for materials with hcp lattice.

Irradiation of material Ti–20Zr in the nanocrystalline state causes the radiation-induced isotropic growth of the grain size to 146 nm (Fig. 2e, f), dislocation of *c*-type doesn't nucleate and anisotropy in the grain distribution is not detected, which testifies

Table 2. Nanohardness (H) and elastic recovery (W) of alloy and coating, before and after irradiation

Samples	Alloy		Coating		
	Initial	After irradiation	As deposited	After annealing	After irradiation
H, GPa	3.7	5.5	8	8	7
W, %	17	–	36	30	23

to the higher radiation resistance of material Ti–20Zr in nanocrystalline state.

Table 2 summarizes the results of the measurements of nanohardness of alloy Ti–20Zr in the microcrystalline and nanostructure state before and after irradiation. As it is seen from the Table the nanohardness of the initial alloy constitutes ≈3.7 GPa. The value of elastic recovery is on the level corresponding to metals and alloys. Nanohardness and elastic recovery of the coating are two times higher than these values for the microcrystalline material; this is caused by its nanosized structure and high internal stresses. Vacuum annealing of the coating causes only a decrease of elastic recovery (by 6 %) at unchanging nanohardness, the grain size is also unchanging. Consequently, the high value of nanohardness is due only to nanosized structure of the coating. After irradiation the increase of the nanohardness of alloy is due to the radiation hardening and some decrease of the nanohardness and elastic recovery is due to the increase of the grain size (see Fig. 3e, f).

4. Conclusions

At exposure of alloy Ti–20Zr in recrystallized state to 80 dpa at 500°C dislocations of c-type are observed; these dislocations are the characteristic sign of accelerated phase of radiation growth. Irradiation of Ti–20Zr material in nanocrystalline state causes the radiation-induced isotropic growth of grain sizes. Dislocations of c-type don't nucleate and anisotropy in the grain distribution testifies to the higher radiation resistance of Ti–20Zr material in the nanocrystalline state. Vacuum annealing of the nanocrystalline material at 500°C during 1 hour doesn't cause the change of the phase composition, of texture, of grain size and also the decrease of nanohardness. The used in our work process of vacuum-arc deposition on the equipment "Bulat" from two oncoming flows of titanium and zirconium plasma allows to produce the nanocrystalline condensates on the base of two metals of required element composition.

References

1. S.S.Ushkov, O.A.Kozhevnikov, *Probl. Mater. Scie.*, **59**, 172 (2009).
2. V.V.Rybin, S.S.Ushkov, O.A.Kozhevnikov, *Probl. Mater. Sci.*, **45**, 159 (2006).
3. R.A.Andrievski, *Phys. Metals and Metallography*, **110**, 243 (2010).
4. S.Wurster, R.Pippan, *Scripta Mater.*, **60**, 1083 (2009).
5. N.Nita, R.Schaeublin, M.Victoria, *J. Nucl. Mater.*, **329–333**, 953 (2004).
6. A.R.Kilmametov, D.V.Gunderov, R.Z.Valiev et al., *Scripta Mater.*, **59**, 1027 (2008).
7. D.Kaoumi, A.T.Motta, R.C.Birtcher, *J.Appl. Phys.*, **104**, 073525 (2008).
8. I.I.Aksenov, V.M.Khoroshikh, N.S.Lomino et al., *IEEE Trans. on Plasma Sci.*, **27**, 1026(1999).
9. Y.S.Umansky, Radiography of Metals and Semiconductors, Metallurgy, Moscow (1969) [in Russian].
10. S.S.Gorelik, J.A.Skakov, L.N.Rastorgouev, X-ray and Electron-optical Analysis, MISA, Moscow (1994) [in Russian].
11. O.M.Barabash, Y.N.Koval, The Crystal Structure of Metals and Alloys, Naukova Dumka, Kiev (1986).
12. A.S.Vus, S.V.Malykhin, A.T.Pygachov et al., *Functional Materials*, **14**, 204 (2007).
13. V.V.Vasil'ev, A.A.Luchaninov, E.N.Reshetnyak et al., *Voprosy Atomnoy Nauki i Tekhniki*, **93**, 173 (2009).
14. M.A.Krivoglaz, The Theory of the Scattering of X-rays and Thermal Neutrons Real Crystals, Nauka, Moscow (1967) [in Russian].
15. A.S.Bakai, A.I.Zhukov, S.N.Sleptsov, *J. Phys.:Condens. Matter.*, **11**, 5681 (1999).
16. Y.D.Yagodkin, S.V.Dobatkin, *Zavodskaya Laboratoriya. Diagnostica Materialov*, **73**, 38 (2007).